PHYSICAL REVIEW B VOLUME 52, NUMBER 18 1 NOVEMBER 1995-II

Large crystalline-induced magnetic anisotropy and field-direction-dependent magnetoresistance in Co($1\bar{1}00$)/Cr(211) superlattices

J. C. A. Huang
Department of Physics, National Cheng-Kung University, Tainan, Taiwan

Y. Liou, Y. D. Yao, W. T. Yang, C. P. Chang, and S. Y. Liao
Institute of Physics, Academia Sinica, Taipei, Taiwan

Y. M. Hu
Department of Physics, National Cheng-Kung University, Tainan, Taiwan

(Received 18 April 1995; revised manuscript received 14 August 1995)

High-quality Co($1\bar{1}00$)/Cr(211) superlattices have been successfully prepared and characterized. Excellent heteroepitaxial (hcp/bcc) growth of Co/Cr superlattices was evidenced by fine streaks in reflection high-energy electron diffraction and superlattice satellites in x-ray diffraction. The magnetic hysteresis loops and magnetoresistance (MR) show strong crystalline-induced magnetic anisotropy and a field-direction-dependent MR effect. We have observed large transverse ($I \perp H$) MR up to about 18% with magnetic field H along the in-plane hard axis Co[$11\bar{2}0$], and current I along the in-plane easy axis Co[0001], and small longitudinal MR (~0.8%) for I∥H∥Co[$11\bar{2}0$]. On the other hand, negligible longitudinal and transverse MR's (<0.1%) were observed for H∥Co[0001].

Magnetotransport properties of magnetic materials have been widely studied for many years.[1] Anisotropic magnetoresistance (AMR $\leqslant 5\%$) in ferromagnetic (F) materials has commonly been observed and applied for magnetoresistive sensors.[2,3] In the past few years, giant magnetoresistant (GMR) phenomena in magnetic multilayers has received much attention both from scientific and advanced technological points of view.[4–7] Note that GMR is quite different from the AMR. GMR generally correlates with the change of spin configuration of successive ferromagnetic layers from antiferromagnetic (AF) coupling to F coupling alignment; while AMR is basically an effect due to the spin-orbital interaction.[3,8] In addition, it has been found that GMR is isotropic for relative direction between the field H and the current I, while AMR depends on relative direction of H and I.

Conventionally AMR is defined by $\Delta R_{\mathrm{AMR}}/R_0 = (R_{\parallel} - R_{\perp})/R_0$, where $R_{\parallel}$ and $R_{\perp}$ are the resistance when the saturated magnetization is parallel and perpendicular to the current, respectively, and $R_0 = (R_{\parallel} + 2R_{\perp})/3$. On the other hand, GMR is generally defined as $\Delta R_{\mathrm{GMR}}/R_{\mathrm{F}} = (R_{\mathrm{F}} - R_{\mathrm{AF}})/R_{\mathrm{F}}$, where R_{F} is the resistance at saturated magnetic field when spins of ferromagnetic layers are in F coupling state; R_{AF} is the resistance at low (coercive) field when the ferromagnetic layers are in AF coupling configuration.

Co/Cr multilayers attracted our attention because of its remarkable structural and magnetic properties, and possible technological applications such as high-density magnetic and magneto-optical recording media. Interestingly, it has been found that Co/Cr (Refs. 9,10) multilayers possess relatively small GMR (less than 5%) compared to the large GMR (over 40%) in Fe/Cr (Refs. 5,6) and Co/Cu (Refs. 7,8) multilayer systems. It is also noted that the magnetic and magnetotransport properties of the magnetic films and multilayers may be strongly affected by the electronic configuration of the films, which in turn depends on their crystal structures.[11–16] There is, however, scant information about the influence of the crystal structure and orientation upon the magnetoresistance (MR) or other magnetic and magnetotransport properties. Previous studies[17–19] on Co/Cr multilayers have often been restricted to polycrystalline, textured, or semiepitaxial samples, making the understanding of the structural and magnetic properties and their interplay more fastidious. One exception is the epitaxial growth of Co($11\bar{2}0$)/Cr(100) superlattices.[20,21] In this multilayer system there still are problems of symmetry (twofold/fourfold) and lattice-spacing (about 5% in one direction) mismatches.[21] High-quality, lattice- and symmetry-matched Co($1\bar{1}00$)/Cr(211) superlattices presented in this work provide us with a model system for the study of the relationship between the structural and magnetic properties.

In this investigation, we report the successful growth and magnetic and magnetotransport studies of heteroepitaxial Co($1\bar{1}00$)/Cr(211) superlattices for the first time to our best knowledge. We have indeed grown more than 30 samples of Co($1\bar{1}00$)/Cr(211) superlattices by molecular beam epitaxy (MBE): $[\mathrm{Co}(40\ \text{Å})/\mathrm{Cr}(t_{\mathrm{Cr}})]_N$ ($2\ \text{Å} \leqslant t_{\mathrm{Cr}} \leqslant 35\ \text{Å}$, $15 \leqslant N \leqslant 20$). We present here mainly the general and common features of these samples, especially stress on the strong magnetic anisotropy and the field-direction-dependent MR effect induced by the well-defined crystallinity.

The Co($1\bar{1}00$)/Cr(211) superlattices were grown on epitaxial grade MgO(110) substrates. Before deposition of the first Cr overlayers of the superlattice, Mo buffer layers of <50 Å were established on the MgO substrates. The initial

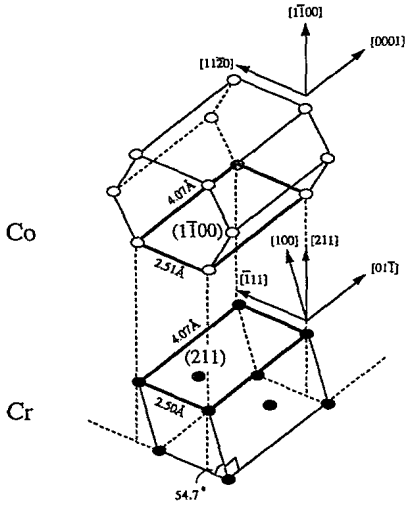

FIG. 1. Schematic diagrams showing the geometry, unit cell (indicated by bold lines), and epitaxial relationship of the bcc Cr(211) and hcp Co(1$\bar{1}$00).

Mo buffer layers were grown at 900 °C ($\sim 0.4T_m$). The subsequent Co/Cr superlattices were grown at 350 °C ($\sim$0.34 T_m). Co, Cr, and Mo (99.99% pure) were evaporated from three separate e-beam evaporators. The growth pressure of superlattices was controlled below 5×10^{-9} Torr, and the deposition rate at $\sim$0.1 Å/s. To enable the growth of high-quality superlattices, MgO substrates were chemically precleaned and rinsed in an ultrasonic cleaner. They were then outgassed at 1000 °C under ultra-high-vacuum conditions for $\sim\frac{1}{2}$ h before initial deposition.

The crystalline orientation and quality were determined by reflection high-energy electron diffraction (RHEED) and x-ray diffraction (XRD). MR and magnetic properties were studied by using a commercial superconducting quantum interference device x-ray diffraction magnetometer in a magnetic field up to 50 kOe with measuring temperature at 10 K. MR measurements were carried out by the conventional four-probe technique with I and H in the plane of the layers. Transverse and longitudinal MR's were measured with $I\perp H$ and $I\|H$, respectively.

For Co(1$\bar{1}$00)/Cr(211) superlattices studied here, we have obtained the following epitaxial relationships: Co(1$\bar{1}$00)‖Cr(211)‖Mo(211)‖MgO(110), Co[11$\bar{2}$0]‖Cr[$\bar{1}$11]‖Mo[$\bar{1}$11]‖MgO[$\bar{1}$10], and Co[0001]‖Cr[0$\bar{1}$1]‖Mo[0$\bar{1}$1]‖MgO[001]. Figure 1 displays the schematic diagrams of the three-dimensional (3D) geometry of the superlattice and the unit cell of the hcp Co(1$\bar{1}$00) and bcc Cr(211). Though Co and Cr possess distinct bulk structures, Co(1$\bar{1}$00) and Cr(211) planes match extremely well in symmetry and lattice parameters. The unit cell of Co(1$\bar{1}$00), 4.07 Å×2.51 Å, matches perfectly with that of Cr(211), 4.07 Å×2.50 Å. This provides us with an unprecedented opportunity to synthesize high-quality heterostructure superlattices.

Typical RHEED patterns of the surfaces of Mo (211) buffer layers, and of Cr(211) and Co(1$\bar{1}$00) layers taken during the growth of the superlattice are shown in Figs. 2(a)–2(c). For a better match to the MgO (110) substrate and hence better growth of the Co/Cr superlattice, the initial Mo buffer layers of about 20 to 40 Å thick are employed. Note that for Mo buffer layers thicker than 100 Å, the Lorentz

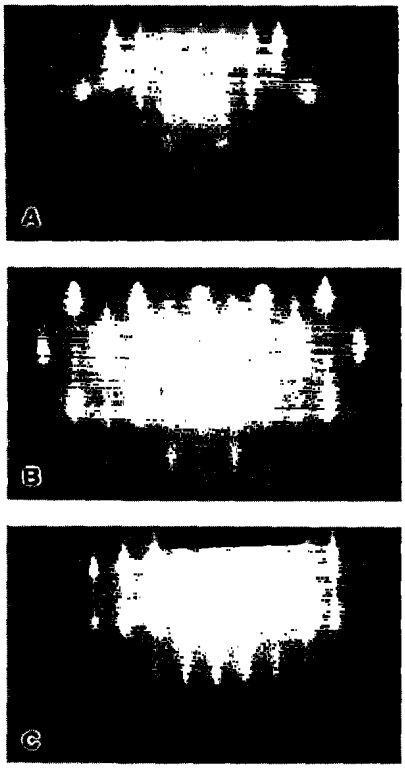

FIG. 2. Typical RHEED patterns of surfaces of the Mo buffer layers and successive Cr and Co layers during the growth of the Co(1$\bar{1}$00)/Cr(211) superlattices showing: (a) Mo(211) along [$\bar{1}$11], (b) Cr(211) along [$\bar{1}$11], and (c) Co(1$\bar{1}$00) along [11$\bar{2}$0].

(positive) MR effect becomes a strong competitive factor at the low temperature of 10 K.[22] As can be seen from Fig. 2(a), Mo buffer layers grow on a nice and atomically flat (211) plane. The following Cr(211) [Fig. 2(b)] and Co(1$\bar{1}$00) overlayers [Fig. 2(c)] remain well ordered but, to some extent, show rougher surfaces due to the relatively low growth temperature of 350 °C, which is, however, the optimal growth temperature for Co/Cr superlattices. From both RHEED and XRD studies, it was found that the bulk and surface order deteriorate for growth temperatures lower than 300 °C. While for growth temperatures above 400 °C the XRD superlatice peaks were strongly suppressed, indicating the significance of the interfacial interdiffusion between Co and Cr layers. Figure 3 shows a typical high-angle XRD spectrum of the Co(1$\bar{1}$00)/Cr(211) superlattices: [Co(40 Å/Cr(20 Å)]$_{20}$. Around the bulk peak positions of Cr(211) and Co(2$\bar{2}$00) [shown by dashed lines in Fig. (3)] several satellite peaks were clearly observed, showing good modulation of the Co and Cr overlayers.

For a series of [Co(40 Å)/Cr(t_{Cr})]$_N$ superlattices, Fig. 4(b) shows the largest measured transverse MR (~18%) at 10 K of the [Co(40 Å)/Cr(15 Å)]$_{18}$ sample for $H\|$Co[11$\bar{2}$0] (hard axis), and $I\|$Co[0001] (easy axis). The longitudinal MR for $I\|H\|$Co[11$\bar{2}$0] is much smaller (~0.8%), as displayed in Fig. 4(a) (MR enlarged by 5 times). For all Co(1$\bar{1}$00)/Cr(211) superlattices studied, the transverse MR's with $H\|$Co[11$\bar{2}$0] and $I\|$Co[0001] are between 8 and 18 % (all negative) and with similar line shapes; while longitudinal MR's with $I\|H\|$Co[11$\bar{2}$0] are from 0 to 1 %. The transverse MR's with $H\|$Co[11$\bar{2}$0] are likely dominated by the AMR effect since the GMR effect is isotropic with respect to the

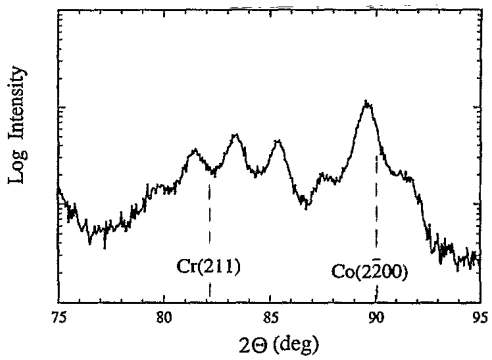

FIG. 3. X-ray-diffraction peaks from the Co(1$\bar{1}$00)/Cr(211) superlattice: [Co(40 Å)/Cr(20 Å)]$_{20}$/Mo(40 Å)/MgO(110). The positions corresponding to the bulk lattice parameters of Cr(211) and Co(2$\bar{2}$00) are indicated by the dashed lines.

relative direction of H and I. The dominance of the AMR effect is further supported by the systematically observations of 5 to 8 % transverse MR's and less than 0.5% longitudinal MR's for various thin Co(1$\bar{1}$00)/Cr(211) bilayer films with H‖Co[11$\bar{2}$0].[23] The dependence of the transverse MR (H‖Co[11$\bar{2}$0]) upon the thickness the Cr spacer layers, however, shows slight oscillation behavior with large background, possibly indicating that the observed MR's are composed of the very small GMR component sitting on top of the large AMR component. This together with the separation of the small GMR (<3%) from the large AMR components are in progress and will be published elsewhere.[24] Shown in Fig. 4(c) is the hysteresis loops for H‖Co[11$\bar{2}$0]. In this field alignment, the saturation field for both MR and magnetization is of about 10 to 15 kOe. The AF-coupling-like hysteresis curve is mainly due to the field along the hard axis (H‖Co[11$\bar{2}$0]) rather than due to the AF coupling effect between the neighboring Co layers, since the coupling effect is weaker than the magnetic anisotropic effect in the Co(1$\bar{1}$00)/Cr(211) multilayer system, as discussed below.

For H‖Co[0001], on the other hand, the corresponding hysteresis measurement shows a nice rectangular loop with a comparatively smaller saturation field of ~700 Oe, as shown in Fig. 5(c). Interestingly, both the transverse and longitudinal MR's are almost completely suppressed (MR≤0.1%), as shown in Figs. 5(a) and 5(b). The above results indicate that for Co(1$\bar{1}$00)/Cr(211) superlattices the MR not only depends on the relative direction of H and I, but also depends strongly on the relative direction of the magnetic field H and the crystalline axis. That is, MR=MR(θ), where θ is the relative direction of H and the in-plane easy axis, Co[0001]. Preliminary results show that transverse MR(θ) increases monotonically with the increasing of θ from 0 (H‖Co[0001]) to $\pi/2$ (H‖Co[11$\bar{2}$0]).

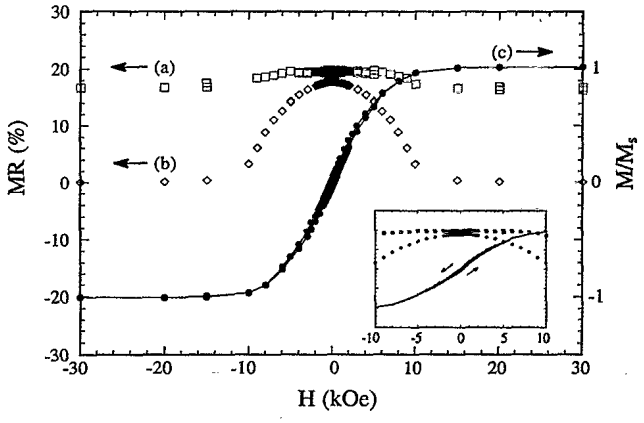

FIG. 4. The magnetization and magnetoresistance as a function of applied magnetic field H‖Co[11$\bar{2}$0] at 10 K for [Co(40 Å)/Cr(15 Å)]$_{18}$ superlattice showing (a) longitudinal MR (I‖H) with the magnitude of MR enlarged by 5 times for clarity, (b) transverse MR ($I\perp H$), and (c) hysteresis loops of magnetization.

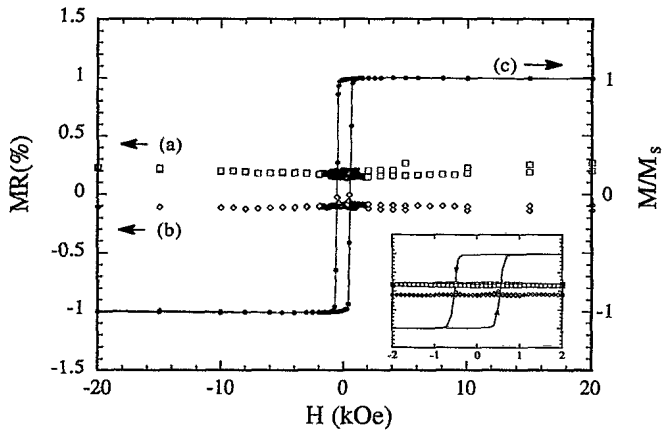

FIG. 5. The magnetization and magnetoresistance as a function of applied magnetic field H‖Co[0001] at 10 K for [Co(40 Å)/Cr(15 Å)]$_{18}$ superlattice showing (a) longitudinal MR (I‖H), (b) transverse MR ($I\perp H$), and (c) hysteresis loops of magnetization.

Note that the strong anisotropic effect mentioned above is also found in the Co/Cr(211) bilayers,[23] but not observed for single Co films (hcp or fcc phase) directly deposited on MgO or the other (sapphires, Si, and GaAs) substrates. It appears that Cr plays a significant role in determining the observed strong anisotropic effect. Nevertheless, we have also observed that the anisotropic effect is negligible for polycrystalline or textured Co/Cr bilayers and multilayers. We therefore conclude that both the Cr element and the (211) plane, which perfectly selects the single hexagonal phase and hence the uniaxial anisotropy of Co(1$\bar{1}$00) layers, are required for the strong anisotropic effect. The fact that MR's are enhanced from less than 8 in bilayers to 18% in multilayers indicating that interfacial scattering between Co and Cr layers could be an important factor compared to the scattering within the ferromagnetic layers. It is possible that some interfacial Cr layers are strongly polarized by the well magnetically ordered Co(1$\bar{1}$00) layers.

Question remains as to why the MR depends so strongly on the relative direction of H and the crystalline axis for multilayers such as hcp/bcc Co(1$\bar{1}$00)/Cr(211) superlattices, in marked contrast to cubic/cubic [e.g., bcc/bcc Fe/Cr (100)(211)[28]] multilayer systems which instead exhibit a stronger coupling effect. Here we make a simple argument based upon the total energy consideration reported in other work.[29] The total energy density (energy per surface area) of the multilayer system can generally be given by $E_{tot}=E_H+E_a+E_c$, where E_H is the field energy density, E_a is magnetocrystalline anisotropic energy density, and E_c is the coupling energy density.

By neglecting the surface anisotropy term for the multilayer, E_a for each Co layer can be approximated as

$-t_{Co}K_u \cos^2\theta$, where $t_{Co}(=40$ Å) is the thickness of Co in one bilayer, K_u is the uniaxial anisotropic constant deciding the strength of anisotropy, and θ denotes the relative direction between the magnetization and the easy axis of Co[0001]. K_u is about 4.5×10^6 erg/cm^3 for bulk Co and therefore $E_a\sim-1.8\cos^2\theta$ (erg/cm^2).[25,26] For $H=H_s=15$ kOe (saturation field for H along the hard axis, see Fig. 4), $M=M_s$ (saturation magnetization $\sim1.43\times10^3$ emu/cc for Bulk Co), the field energy density is given by $E_H=-HM_st_{Co}\sim-1.8$ (erg/cm^2). This amount of field energy can just balance the (magnetocrystalline-induced) anisotropic energy.

For comparison, the interlayer coupling energy density is given by $E_c=J_c\cos(\Delta\phi)$, where J_c is the coupling strength and $\Delta\phi$ is the relative direction of the magnetization of the successive ferromagnetic layers. $J_c>0$ ($J_c<0$) if the neighboring Co layers are AF (F) coupled. The maximum AF coupling strength (if $J_c=J_{AF}>0$) of neighboring Co layers through Cr spacer layers is estimated by $E_c\sim-J_{AF}\cos(\pi)\sim-0.24$ (erg/cm^2) for the first AF coupling peak.[27] Possibly due to the dominance of the anisotropic effect $\{\Delta E_a\sim-1.8[\cos^2(\pi/2)-\cos^20]=1.8$ erg/cm$^2\}$ over the interlayer coupling effect $[\Delta E_c\sim J_{AF}\cos(0)-J_{AF}\cos(\pi)\sim0.48$ erg/cm$^2]$ and the field effect at low field, the magnetic and magnetotransport properties of Co(1$\bar{1}$00)/Cr(211) superlattices display strong anisotropic behavior.

The strong influence of the strong crystalline to the magnetotransport properties discussed above is diminished or eliminated in a cubic system such as bcc Fe/Cr(100) or in polycrystal multilayers. The peculiarity of the Co(1$\bar{1}$00)/Cr(211) system in that there is a well defined, strong (in-plane) uniaxial anisotropy for hexagonal Co layers and hence a unique easy axis for magnetization. Indeed, it is found that all of our Co(1$\bar{1}$00)/Cr(211) superlattices possess large remanent magnetization even before applying the magnetic field, and cannot be demagnetized (up to about 3 kOe demagnetization field at room temperature) using standard demagnetizing procedures by applying oscillatory damped currents to the electromagnets to these samples. That is to say, the Co(1$\bar{1}$00)/Cr(211) superlattices behave as very large domain-like crystals, indicating the excellence of the atomic and magnetic ordering of the samples. On the other hand, there are two ([010] and [001] of Fe) or more (polycrystallines) equivalent easy axes for cubic Fe/Cr(100), and thus more complicated multidomains can usually be formed for cubic systems at low field. There is no more unique sense for domain alignment and motion. Even for Fe/Cr(211) systems which show strong in-plane magnetic anisotropy, strong AMR effects have not been observed.[28] This could be due to the smallness of the anisotropy energy of Fe (Ref. 25) (by about a factor of 10 smaller) compared to that of hcp Co. The anisotropic effect in Fe/Cr multilayer and many other cubic/cubic systems could thus be insignificant compared to their interlayer coupling effect, and the GMR effect can therefore become a controlling factor.

In summary, we have reported the epitaxial growth and the structural and magnetic characterizations of Co(1$\bar{1}$00)/Cr(211) superlattices. The magnetic hysteresis loops and MR show strong crystalline-induced magnetic anisotropy and field-direction-dependent MR effects. The strong in-plane magnetic anisotropy is a result of the well-defined hexagonal crystallininity of the Co(1$\bar{1}$00) layers, which are epitaxially selected by the Cr(211) planes. The large AMR effect could be due to the scattering both from the Co layers and the Co/Cr interfacial layers. Detailed analyses of the magnetic and magnetotransport properties of the Co(1$\bar{1}$00)/Cr(211) superlattices, such as the dependence of the MR upon the thickness of Co layers and Cr spacer layers, and temperature dependence of MR, are all under intensive study and will be published elsewhere.

We are grateful for the financial support by the ROC NSC under Grant Nos. 84-2112-M-006-017, 84-2112-M-006-018 (J.C.A.H.), 84-2112-M-001-039 (Y.L.), and 84-2112-M-001-042 (Y.D.Y.).

[1] See, for example, *Magnetoresistance in Metals*, edited by A. B. Pippard (Cambridge University Press, Cambridge, 1989).
[2] P. Ciureanu, in *Thin Film Resistive Sensors*, edited by P. Ciureanu and S. Middelhoek (Institute of Physics and Physical Society, Bristol, 1992), p. 253.
[3] T. R. Mcguire and R. I. Potter, IEEE Trans. Magn. **MAG-11**, 1018 (1975).
[4] M. N. Baibich *et al.*, Phys. Rev. Lett. **61**, 2472 (1988).
[5] E. E. Fullerton *et al.*, Appl. Phys. Lett. **63**, 1699 (1993).
[6] S. S. P. Parkin *et al.*, Appl. Phys. Lett. **58**, 2710 (1991).
[7] S. S. P. Parkin *et al.*, Phys. Rev. Lett. **66**, 2152 (1991).
[8] J. Smit, Physica (Utrecht) **XVI**, 612 (1951).
[9] S. S. P. Parkin *et al.*, Phys. Rev. Lett. **64**, 2304 (1990).
[10] Y. Liou *et al.*, J. Appl. Phys. **76**, 6516 (1994).
[11] G. A. Prinz, Phys. Rev. Lett. **54**, 1051 (1985).
[12] D. P. Pappas *et al.*, Phys. Rev. Lett. **64**, 3179 (1990).
[13] F. J. A. den Broeder *et al.*, Phys. Rev. Lett. **60**, 2769 (1988).
[14] E. E. Fullerton *et al.*, Phys. Rev. Lett. **68**, 859 (1992).
[15] K. Le Dang *et al.*, Appl. Phys. Lett. **63**, 108 (1993).
[16] A. R. Modak *et al.*, Phys. Rev. B **50**, 4232 (1994).
[17] D. Wang and D. J. Sellmyer, J. Appl. Phys. **69**, 4541 (1991); D. Wang *et al.*, *ibid.* **73**, 6353 (1993).
[18] M. B. Sterns *et al.*, Phys. Rev. B **40**, 8256 (1989); M. B. Sterns *et al.*, J. Appl. Phys. **67**, 5925 (1990).
[19] Y. Henry *et al.*, Phys. Rev. B **47**, 15 037 (1993).
[20] W. Donner *et al.*, Phys. Rev. B **48**, 14 745 (1993).
[21] J. C. A. Huang *et al.*, J. Cryst. Growth **139**, 363 (1994).
[22] J. C. A. Huang *et al.*, Appl. Surf. Sci. (to be published).
[23] Y. D. Yao *et al.* (unpublished).
[24] Y. Liou *et al.* (unpublished).
[25] *Introduction to Magnetism and Magnetic Materials*, edited by D. Jiles (Chapman and Hall, London, 1991), p. 134.
[26] K_u is usually enhanced (by a factor from 1 to 3) in Co/TM multilayers, see for example, *Ultrathin Magnetic Structures*, edited by J. A. C. Bland and B. Heinrich (Springer-Verlag, Berlin, 1994), p. 80.
[27] S. S. P. Parkin, Phys. Rev. Lett. **67**, 3598 (1991).
[28] E. E. Fullerton *et al.*, Phys. Rev. B **48**, 15 755 (1993).
[29] W. Folkerts, J. Magn. Magn. Mater. **94**, 302 (1991).